UNIVERSITY OF TROMSØ UIT

FACULTY OF SCIENCE AND TECHNOLOGY
DEPARTMENT OF PHYSICS AND TECHNOLOGY

Ice Shelf - Ocean Interaction in the Eastern Weddell Sea, Antarctica

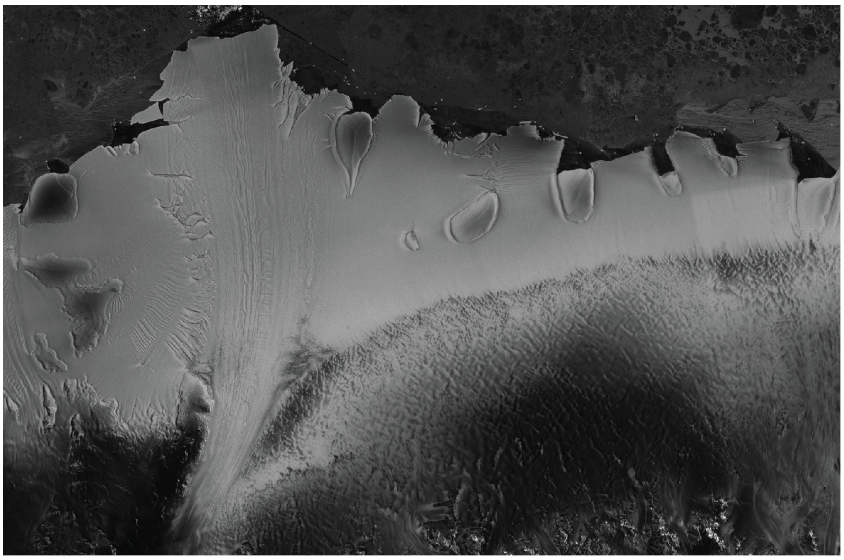

TORE HATTERMANN

A dissertation for the degree of
Philosophiae Doctor

October 2012

NORWEGIAN POLAR INSTITUTE

CENTRE FOR ICE, CLIMATE AND ECOSYSTEMS

Acknowledgements

This dissertation would not have been possible without the inspiring and free-thinking, but yet targeted and scientifically sound support of Ole Anders, who has been a great supervisor throughout my time at the Norwegian Polar Institute–Thank you! Also Jonathan, who patiently exercised the trans-Atlantic supervision of my PhD-project, as well as Lars Henrik, who at times was my closest sparring-mate for scientific discussion, tremendously contributed to the results of this work and the personal progress of my research career. I want to thank Elisabeth, Nalân and Sebastian who were my administrative principals at the Polar institute for their goodwill and their honest interest in my work, and also Alfred who has been a supportive and encouraging supervisor at the University of Tromsø, even though the topic of my PhD is only remotely linked to his field of expertise. Beyond that I am grateful to the many souls who were with me during the last three years, helping to get out of the many smaller and larger pitfalls along the way: the great colleagues at the Polar Institute, in particular Qin my office mate and closest fellow, as well all the other conspirative students at the end of the corridor, and the cheerful sofa-lunch-eaters and coffee-breakers who made (office) life a lot more colorful; the creative minds of the Fimbul– Top-to-Bottom project who were great to be with in the bureau as well as during three fantastic field seasons on the Fimbul Ice Shelf, or surfing the waves of the Pacific; but also the tough girls and boys at Troll doing a passionate and stunning job, facilitating excellent conditions for science in Antarctica. The work on this thesis also lead me into an interesting research community, where I found precious network of teachers and colleagues, which I am grateful and proud to be part of. Finally, I want thank the people who were with me during the last three years, and supported my work without any professional interest: the good friends I found in Tromsø, especially my flatmates who tolerated my narcissistic obsession for ice shelf- ocean processes; the cherished people in Germany who I met unfortunately far too seldom in the past; my dear family who was supportive and giving, despite the fact of Tromsø being distant from their home in many ways. And then there are you, my beloved Anne. You first motivated me to come to Norway and then I made you to having to bear with me throughout this PhD thing. You do not only deserve my deepest gratitude, but also my apologizes for all the hassle. Now it's finally done and I am looking forward to depart into the next exciting adventure together with you!

Tromsø, October 2012
Tore Hattermann

Abstract

This thesis investigates the interaction of the Antarctic ice shelves along the coast of Dronning Maud Land with the ocean circulation in the Eastern Weddell Sea. A set of direct oceanic observations below the Fimbul Ice Shelf, which were acquired during three Antarctic field seasons in the austral summers 2009/10, 2010/11 and 2011/12, is a central element of the presented work. This new oceanographic dataset is complemented by a high-resolution state-of-the-art ice shelf - ocean circulation model. The results provide an estimate of the amount of basal melting at the Fimbul Ice Shelf, and revise the physical processes that determine the ocean heat fluxes over the East Antarctic continental slope. A major finding is that deep-ocean heat fluxes towards the ice are much more constrained than predicted by previous ocean models, causing substantially lower rates of basal melting than earlier suggested. The predicted basal melting is consistent with mass balance estimates from satellite data and implicates that the Fimbul Ice Shelf is currently not subject to rapid basal mass loss. Furthermore, the complex interplay of the processes within the coastal, frontal system, and their respective role in transporting heat for melting towards the ice is examined. The results emphasize the importance of oceanic eddies within the coastal circulation for controlling the inflow of Warm Deep Water into the ice shelf cavities. A realistic representation of the effect of the mesoscale eddy overturning is thus a crucial requirement in order to simulate basal melting along the Weddell Sea coast in the present and future climate. The results also imply that fresh, and solar-heated Antarctic Surface Water plays a central role for the ice shelf cavity exchange. Being produced by sea ice melting at the ocean surface, this water mass directly enters the cavity and increases the melting of shallow ice. Due to its buoyancy, the presence of Antarctic Surface Water also alters the coastal dynamics and regulates the inflow of warm water at depth, thus showing that a more detailed understanding of the role of this water mass for basal melting around Antarctica will need further attention. Finally, the results suggest a direct relationship between the simulated basal melting and only a few deterministic parameters of the coastal circulation, which is used to derive a simple parameterization of for basal melting at the Fimbul Ice Shelf.

List of papers

O. A. Nøst, M. Biuw, V. Tverberg, C. Lydersen, T. Hattermann, Q. Zhou, L. H. Smedsrud, and K. M. Kovacs, 2011. Eddy overturning of the Antarctic Slope Front controls glacial melting in the Eastern Weddell Sea. Journal of Geophysical Research

T. Hattermann, O. A. Nøst, J. M. Lilly, and L. H. Smedsrud, 2012. Two years of oceanic observations below the Fimbul Ice Shelf, Antarctica. Geophysical Research Letters

T. Hattermann, L. H. Smedsrud, O. A. Nøst, J. M. Lilly, and B. Galton-Fenzi, 2012. Modeling basal melting below the Fimbul Ice Shelf, Antarctica. A manuscript in preparation.

Q. Zhou, T. Hattermann, O. A. Nøst, 2012. Wind-driven spreading of fresh Antarctica Surface Water below ice shelves in the Eastern Weddell Sea. A manuscript in preparation.

Abbreviations and Glossary

ASF	Antarctic Slope Front, separating the Warm Deep Water below the continental shelf break and the colder Eastern Shelf Water, comprising substantial horizontal density gradients
ASW	fresh and warm Antarctic Surface Water, produced by solar heating and melting of sea ice during summer
baroclinic current	vertically sheared current
barotropic current	vertically uniform current
buoyancy	upward or downward force due to gravity acting on a parcel of water that is more or less dense than other water at its level
CTD	Conductivity, Temperature, Depth–oceanographic standard measurement
ESW	Eastern Shelf Water, residing on the Eastern Weddell Sea continental Shelf with temperatures close to the surface freezing point
EWS	The Eastern Weddell Sea region
FIS	The Fimbul Ice Shelf
geostrophy	dynamical steady state of a fluid moving perpendicular to a pressure gradient, which is balanced by the Coriolis force
ISW	Ice Shelf Water, produced by the ice - ocean interaction at greater depth, characterized by temperatures below the surface freezing point
meridional	along a meridian, north-south
MWDW	Modified Warm Deep Water, originating through mixing within the Antarctic Slope Front - thermocline
ROMS	The Regional Ocean Modeling System presented by Shchepetkin and McWilliams (2005)
thermocline	oceanic interface between two water masses with a large vertical temperature gradient, in the ASF coinciding with a large vertical density gradient
WDW	Warm Deep Water, residing in the deep-ocean below the Eastern Weddell Sea continental shelf with a temperature maximum of about 0.9°C
zonal	along a latitude, east-west

Contents

Part I

Summary

1 Introduction

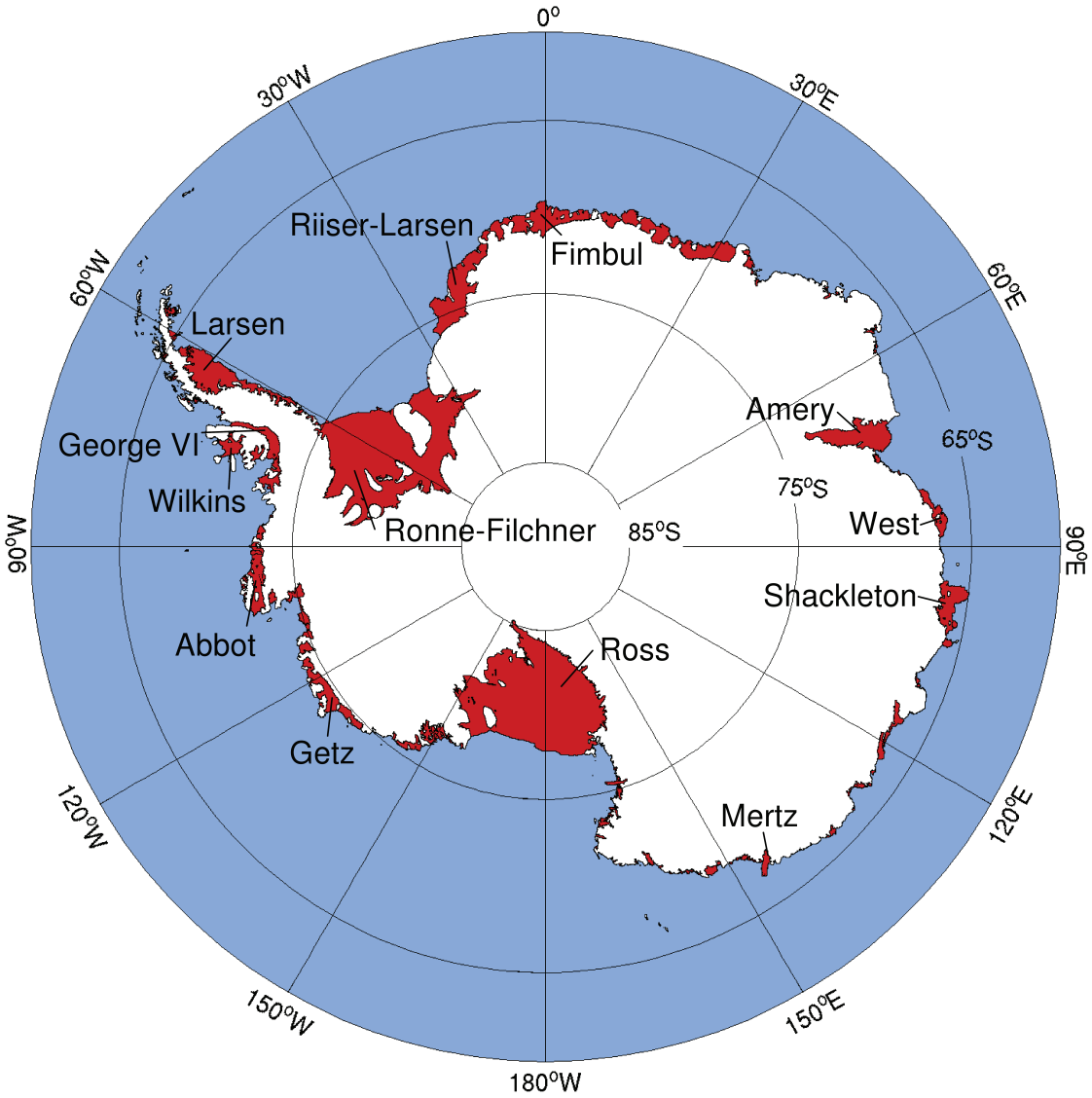

Figure 1.1: *A map of Antarctica borrowed from Galton-Fenzi (2009), showing the grounded ice sheet (white) with its floating extensions, the Antarctic Ice Shelves (red), the direct interface between the Antarctic glacier ice and the Southern Ocean (blue).*

The work presented in this dissertation is aimed at contributing a better understanding of basal melting of the ice shelves in Antarctica. Ice shelves are the floating extension of the grounded Antarctic Ice Sheet (Figure 1.1). They cover about half of the Antarctic coast, being the interface between the glaciated continent and the Southern Ocean. Due to cold air temperatures, most of the precipitation that falls over Antarctica is transformed into glacier ice, and approximately 80 % of all mass that is lost from the ice sheet is drained into the ice shelves, where it is ultimately released into the ocean by either calving (break-off of icebergs) or melting at the ice - ocean interface (Jacobs et al., 1992).

Apart from comprising an interesting and challenging interplay of physical processes, basal ice shelf melting is believed to play an important role in the global climate system. The production of glacial melt water due to basal melting releases a substantial amount of fresh water into the ocean, which is believed to have an important effect on the global circulation (Fahrbach et al., 1994). Furthermore, the ice sheet - ice shelf - ocean interaction directly controls the Antarctic mass balance (Joughin and Alley, 2011; Pollard and DeConto, 2009) and thus the evolution of the global sea level. Although being only marginally affected by the melting of floating ice, sea level changes are believed to be regulated by the presence of the Antarctic ice shelves, which act to hold back the flow of grounded glacier-ice into the Southern Ocean (Dupont and Alley, 2005).

The recent increase in global temperatures and the observation of rapid changes around Antarctica (Scambos et al., 2000) have raised concerns about the future evolution of the Antarctic ice shelves in a changing climate (Solomon et al., 2007). Observations documented the increasing glacial mass discharge after the sudden collapse of large ice shelf areas along the Antarctic Peninsula (Scambos et al., 2004). In western Antarctica, evidence is growing that the observed increased glacial mass loss may have been triggered by changes in deep-ocean heat fluxes towards the glaciated coast (Pritchard et al., 2012; Jacobs et al., 2011). Furthermore, future projections of continental-scale climate models suggest that changing ocean circulations may cause drastic increase of basal melting in parts of eastern Antarctica within this century (Hellmer et al., 2012).

Experiencing progressively more attention within the research community, the understanding of the ice shelf - ocean interaction has significantly increased within the recent years. Especially the rapid development, of satellite-based remote sensing techniques that provide diagnostic estimates of the ice shelf mass balance on continental scales (Rignot et al., 2008), is a tremendous achievement. However, large gaps remain to be filled when estimating basal melting in a predictive way, i.e., by quantifying the amount of oceanic heat that reaches the ice, and how this might change in a future climate (Pritchard et al., 2012). Direct observations below the several hundred meter thick ice shelves are sparse, and the incorporation of ice shelf - ocean processes into global climate models is hampered by incompatibility of time and grid scales. Yet, the heat supply for basal melting is determined by a complex interplay of oceanic and atmospheric processes, being particular for the coastal region (Smedsrud et al., 2006; Thoma et al., 2008; Nicholls, 1997).

This study investigates the oceanic processes controlling basal melting in the Eastern Weddell Sea (EWS hereafter), with a primary focus on the Fimbul Ice Shelf (FIS hereafter), which represents the typical configuration of ice shelves in this region. By combining a

suite of ocean observations with oceanographic theory and numerical circulation modeling, the following two main-objectives are addressed:

1. Which water masses access the ice shelf cavity, and how large is the amount of basal melting at the FIS?

2. Which are the important oceanic processes that control the ice shelf - ocean heat exchange in the EWS, and how do those respond to varying climatic conditions?

Beside its general relevance for determining the overall mass balance of the FIS, the first objective is important because previous ocean modeling studies (Hellmer, 2004; Smedsrud et al., 2006) disagree with remote sensing mass balance estimates (Rignot et al., 2008) and suggested the possibility of a rapid basal mass loss scenario for the ice shelves of the EWS. After several observational studies already indicated that the models were wrong (Nicholls et al., 2006; Price et al., 2008), the work presented here finally proves that melt rates at the FIS are low, and that the such a rapid basal mass loss scenario is presently unlikely to happen below the FIS. This *a fortiori* emphasizes the need to better understand the underlying dynamics, in order to improve the predictions of ice shelf basal melting in the present and future climate. Another motivation for studying basal melting in the FIS region is the availability of a rich collection of measurements which allows to design a concise and consistent numerical model that may directly be evaluated by observations, in order to validate the results.

Over the scope of three years, the investigation of these objectives has lead to four manuscripts on the topic of ice shelf - ocean interaction in the Eastern Weddell Sea, which are the main pillars of this dissertation and being presented in **Part II** of the document. By the time of submission of this thesis, two of the papers are already published in high-quality international peer-review journals, whereas the remaining two manuscripts are presented in an advanced draft version. The remaining of **Part I** of the thesis is structured as follows:

Chapter 2 provides some background information by briefly reviewing the physics of the ice shelf cavity circulation, introducing the characteristics of the EWS region, and presenting the field-work that was carried out as part this study.

Chapter 3 presents the results of this study. The results of the individual papers are summarized in section 3.1 to section 3.2. As an overall summary of their findings, section 3.5 presents a simple parameterization for basal melting below the FIS, which is derived form the model results of Paper 3 and based on the one-dimensional plume model presented in section 2.1.3.

Chapter 4 presents the overall discussion and conclusion of this dissertation.

2 Background

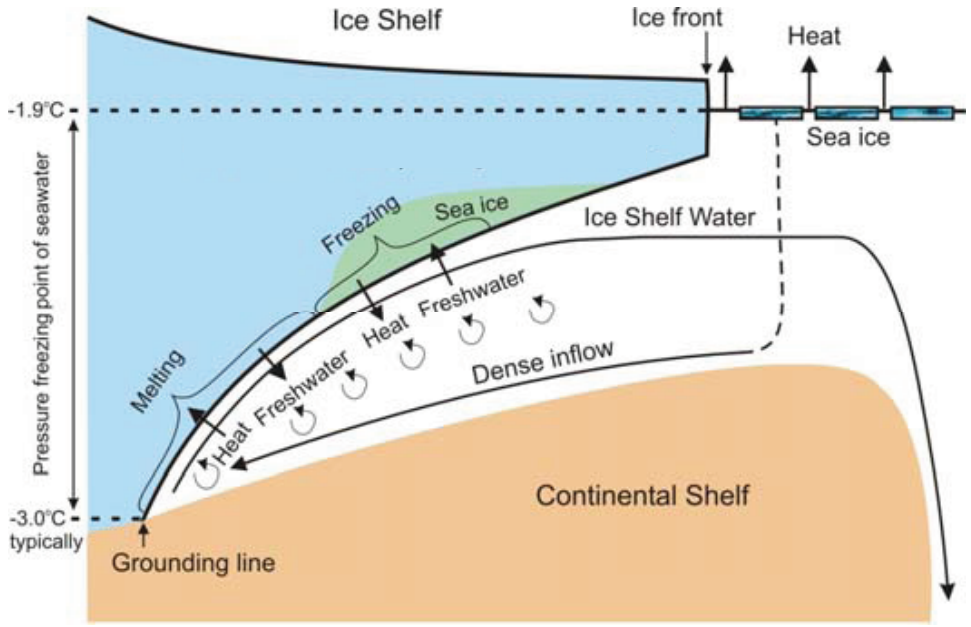

Figure 2.1: *A schematic of the ice pump mechanism. Cold and dense water formed during sea ice production causes basal melting at the grounding line where the pressure dependent freezing point is depressed to lower temperatures. The injected melt water initiates a buoyant plume of Ice Shelf Water that rises along the ice base, and eventually refreezes or leaves the cavity at shallower depth. The figure is taken from Jenkins (2010).*

2.1 The Ice Shelf Cavity Circulation

2.1.1 The Ice-Pump Mechanism

The caverns below the ice shelves are a unique oceanographic environment on Earth. Several hundred meters of ice overlying the ocean affect the sub-shelf circulation. The interaction of seawater with glacier ice at depth induces a characteristic thermohaline circulation (Lewis and Perkin, 1986). The freezing point of seawater decreases with increasing pressure, at a rate of approximately 0.75 °C per kilometer (Jacobs et al., 1992). In this way, even water with temperatures at the surface freezing point (about -1.9 °C) may provide heat to melt ice at depth, producing Ice Shelf Water (ISW hereafter), a mixture of glacial melt water and seawater colder than the surface freezing point, which is exclusively formed in these environments. Gade (1979) shows that seawater which melts ice transforms at a constant ratio of cooling and freshening. This leads to the fundamental principle taht ISW is more buoyant than its source water mass causing the melting, because the density of seawater is to a leading order determined by its salinity at temperatures near the freezing point.

This gives rise to the so called "ice-pump circulation" (Lewis and Perkin, 1986) sketched in Figure 2.1: Cold ISW initiates at the grounding line, the deepest point of the ice

shelf, where the grounded ice sheet becomes afloat. Due to its increased buoyancy, the ISW ascends along the sloping ice base. When reaching shallower depth where the pressure decreases, the ISW with temperatures below the surface freezing point becomes supercooled, and refreezing processes will take place. In this way, the circulation below the ice shelf acts as a heat engine, moving ice from deeper parts of the ice base to shallower depth, and thus lowering the potential energy of the ice - ocean system. However, while rising along the ice base, the ISW continuously mixes with warmer water form the ambient ocean. Therefore, not all the melted ice will refreeze, causing a net mass loss of ice shelf. The efficiency of the ice-pump strongly depends on the geometrical configuration of the individual ice shelf and the properties of the ambient ocean water in the ice shelf cavity. Buoyant plumes of cold ISW originating at the grounding line may reach all the way to the ice front, or in a sufficiently stratified ocean, detach from the ice base and become part of the interior cavity circulation, when being equally buoyant with the ambient water.

2.1.2 Three Modes of Heat Supply for Basal Melting

One objective of this study is to determine the dominant source of oceanic heat that determines the melting below the ice shelves in the EWS. Jacobs et al. (1992) present an extensive and foresighted review of the heat supply below the Antarctic ice shelves, sketching three possible modes of melting.

In mode 1, only water with temperatures at the surface freezing point enters the ice shelf cavity, and the heat supply for melting entirely relies on the presence of an ice-pump circulation. In many areas around Antarctica, the source water for this circulation is dense and saline water mass that originates at the ocean surface due to brine release during the production of sea ice. Overall melt rates in this "freezing point-depression mode"are generally rather low, and substantial basal mass loss occurs usually at deeper parts of the ice base, with significant amounts refreezing of marine ice at shallower parts of the ice shelf.

The other two modes of ice shelf basal melting suggested by Jacobs et al. (1992) refer to melting caused by direct access of an external warm water source below the ice. In mode 2, heat is supplied by relatively warm water of the interior Southern Ocean, which circulates at intermediate depth along the Antarctic continental shelf break. The efficiency of this mode is largely determined by the exchange processes over the continental slope, where water masses are separated by narrow fronts, comprising horizontal temperature gradients of several centigrades over distances of a few tens of kilometers (Rintoul et al., 2001). This mode is believed to bear the largest potential for ice shelf basal melting, as it involves the direct access of water that is substantially warmer than the surface freezing temperature below the ice (Jacobs et al., 1992).

Mode 3 refers to the interaction of surface water with the ice front and shallower parts of the ice base. In this circulation, ocean currents at the ice front enhance the ventilation of the upper parts of the cavity, and seasonally warmer waters of the coastal current may replace the the ISWthat reaches the shallow part of the ice base in a purely mode 1-type circulation.

2.1.3 The Ice Shelf-Plume Model

This section presents a model of the ice shelf cavity circulation, that will be used in section 3.5 to derive a simple basal melting parameterization below the FIS, which, based on a few parameters, reproduces the melt rates that are simulated by the three-dimensional high-resolution general circulation model presented in Paper 3.

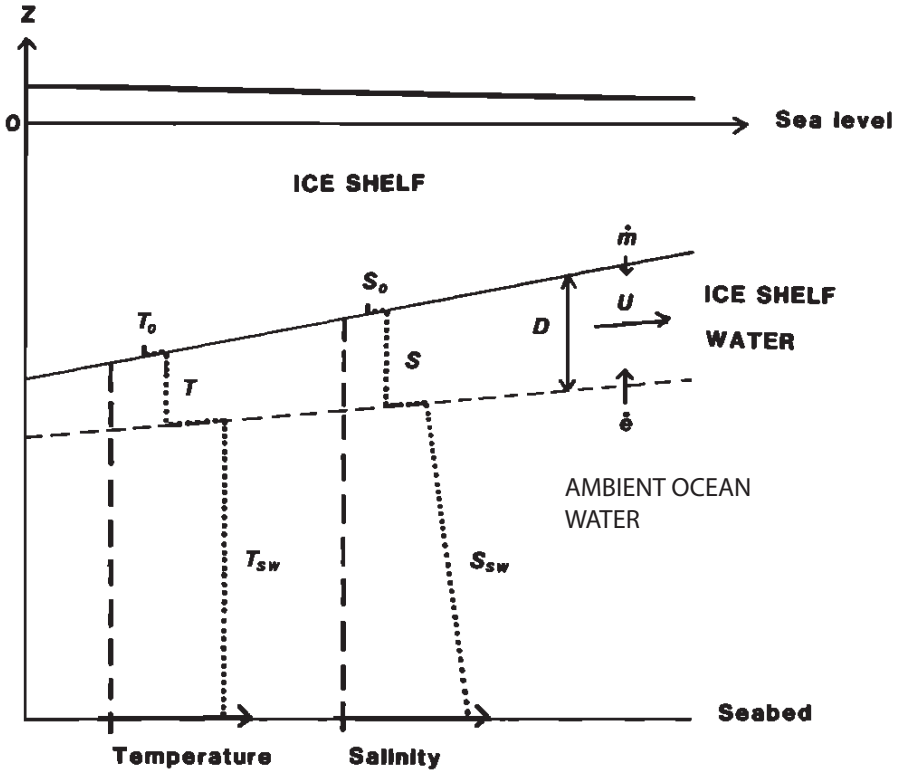

Figure 2.2: *Configuration of the one-dimensional ice shelf-plume model (Jenkins, 1991) showing temperature and salinity through the two layer system.*

Although being driven by entirely different heat sources, all three modes presented in section 2.1.2 have in common that ice shelf basal melting produces buoyant ISW near the ice base. Jenkins (1991) proposed to describe this fundamental feature of the ice shelf cavity circulation by applying the dynamics of a turbulent up-side-down gravity plume that rises along the sloping base of the ice shelf. In this model, which is depicted in Figure 3.7 the ocean is treated as a two-layer system, with the ambient water filling most of the cavity and the plume of ISW being an upper mixed layer below the ice shelf. Turbulence within the gravity-driven flow entrains water from the ambient ocean into the plume, and at the ice shelf base the plume interacts through a turbulent boundary layer for heat and salt. The plume is characterized by a thickness D and depth-averaged values of velocity U, temperature T, and salinity S, parameterized along a one-dimensional path x along

the sloping ice base. Starting at the grounding line, the plume may follow the prescribed path across the ice shelf, ending at the ice front, or it may detach from the ice base when becoming equally buoyant with the ambient water.

Using the same notation as Jenkins (1991), this yields the following equations for conservation of mass, momentum, heat and salt:

$$\frac{d\,(UD)}{dx} = \dot{e} + \dot{m} \tag{2.1}$$

$$\frac{d\,(U^2D)}{dx} = -D\Delta\rho\; g \sin\Theta - KU^2 \tag{2.2}$$

$$\frac{d\,(TUD)}{dx} = T_{SW}\dot{e} + T\dot{m} + (T_0 - T)\,\gamma_T \tag{2.3}$$

$$\frac{d\,(SUD)}{dx} = S_{SW}\dot{e} + S\dot{m} + (S_0 - S)\,\gamma_S \tag{2.4}$$

For the conservation of mass (equation 2.1), the Boussinesq-approximation is applied, with UD being the total transport through a cross-section of the plume, and the melt ($\dot{m}$) and entrainment ($\dot{e}$) rates describing the volume flux across the upper and lower boundary of the plume layer. In the momentum equation 2.2 the first term on the right hand side describes the buoyancy force, with the local density contrast $\Delta\rho$ between the plume and the ambient water, being derived from a linear equation of state. g is the acceleration due to gravity and Θ describes the slope of the ice base. The second term on the right hand side of equation 2.2 describes the frictional drag at the ice - ocean interface with the quadratic drag-coefficient K. In the conservation of heat (equation 2.3) and salt (equation 2.4) T_{SW} and S_{SW} describe the respective temperature and salinity of the ambient ocean. T_0 and S_0 are the corresponding properties at the ice - ocean interface, with γ_T and γ_S being velocity dependent turbulent transfer coefficients for heat and salt.

The turbulent entrainment rate is given as a function of plume velocity and of the slope of the ice base:

$$\dot{e} = E_0 U \sin\Theta, \tag{2.5}$$

with E_0 being a dimensionless constant. The melt rate as well as the temperature and the salinity at the upper-ocean boundary is derived from the balance of heat and salt at the ice - ocean interface as described by Hellmer and Olbers (1989).

This yields a set of four ordinary differential equations, which may be solved numerically for a given ice shelf geometry and ambient ocean properties, using standard methods with little computational effort.

2.2 Ice Shelves in the Eastern Weddell Sea

A comprehensive overview of coastal processes and water masses in the EWS is provided by Nicholls et al. (2009). This section briefly summarizes the main mechanisms that control the interaction of the deep-ocean with the water masses on the continental shelf, which will be the subject of this study.

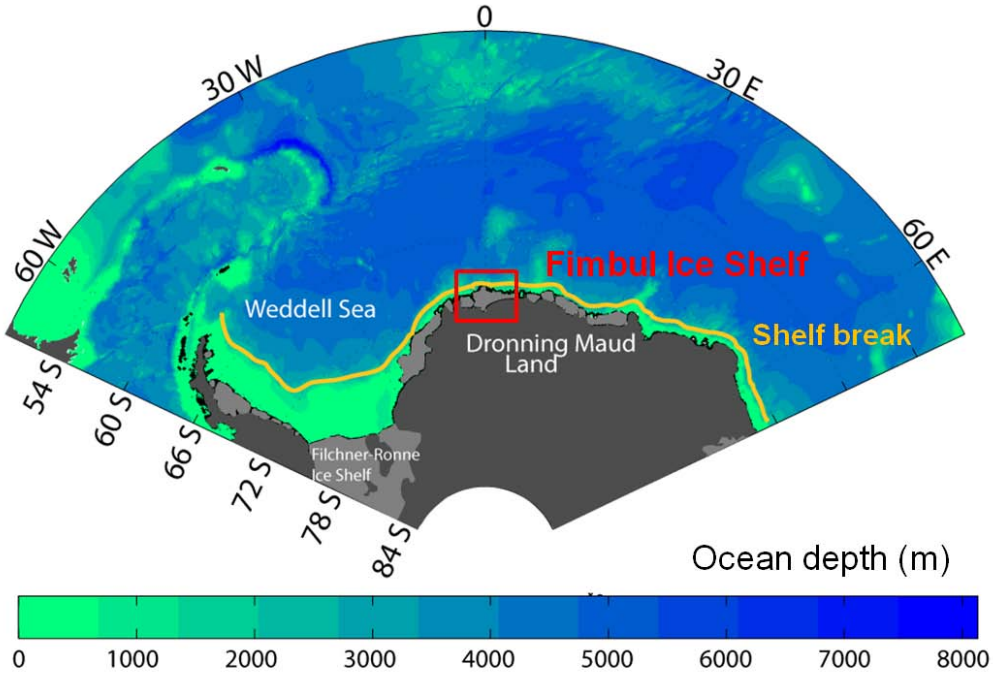

Figure 2.3: *A map of the Weddell Sea and Southern Ocean bathymetry. Light gray areas around the Antarctic coast illustrate the floating ice shelves, with the Fimbul Ice Shelf being indicated by the red rectangle. The yellow line indicates the position of the continentals slope, which runs close to the ice front of the ice shelves in the Eastern Weddell Sea.*

A map of the Weddell Sea bathymetry is shown in Figure 2.3. In the eastern part, along the coast of Dronning Maud Land, ice shelves cover large parts of the narrow continental shelf. Due to their vicinity to the continental slope depicted by the yellow line, basal melting of the ice shelves in this sector of Antarctica is directly controlled by the dynamical processes of the Antarctic Slope Front (ASF hereafter). This frontal system separates the cold Eastern Shelf Water (ESW hereafter) on the continental shelf from the Warm Deep Water (WDW hereafter) residing in the deep-ocean below the continental shelf break (Heywood et al., 1998; Chavanne et al., 2010).

A schematic cross section of the ASF is shown in Figure 2.4. The largest potential heat source for ice shelf basal melting is provided by the WDW, with a temperature maximum of about +0.9 °C. The direct access of this warm water mass to the ice shelf cavity would

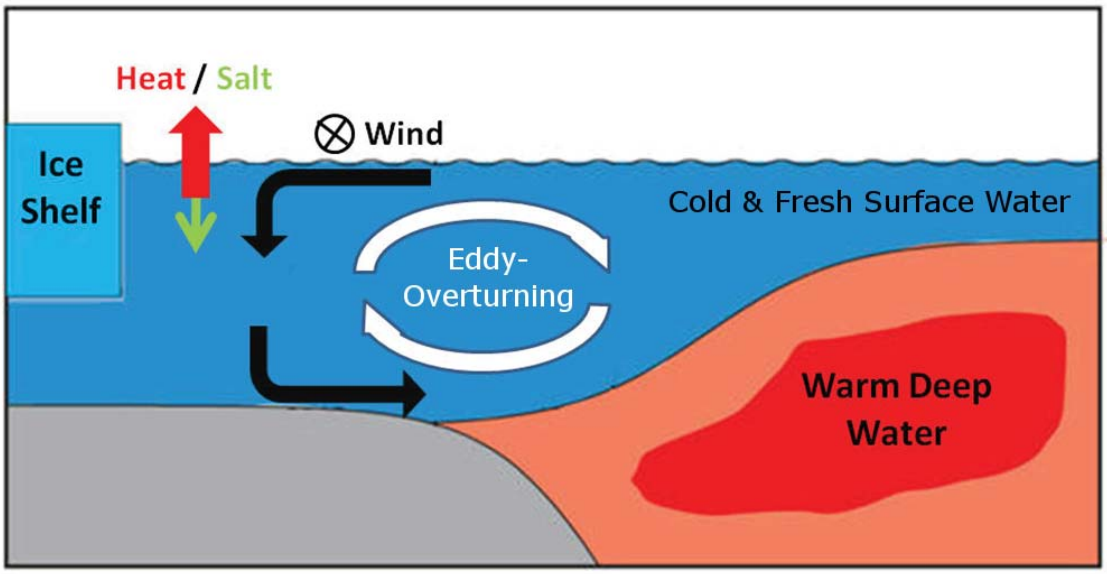

Figure 2.4: *A schematic of the Antarctic Slope Front-processes along the EWS coast. The wind-induced Ekman overturning (black arrows) accumulates fresh surface water over the continental shelf and depresses the denser Warm Deep Water below the shelf break depth. The frontal density contrast induces eddy fluxes (white arrows) that counteract the Ekman overturning. Surface salinity and temperature near the ice edge are largely determined by the seasonal cycle of sea ice freezing and melting.*

cause efficient melting by the mode 2-type circulation described in section 2.1 (Hellmer, 2004; Smedsrud et al., 2006). The WDW is separated from the ESW near the coast by a sloping interface (thermocline), with water masses on the continental shelf being fresher (and therefore less dense) with temperatures being permanently near the surface freezing point.

A first description of the coastal momentum balance of the ASF is provided by Sverdrup (1953), suggesting the wind-driven Ekman overturning illustrated in Figure 2.4 to be the main mechanism that sets up the front. In this picture, wind is the main source of kinetic energy, blowing predominantly from the east along the coast. The induced momentum is balanced by the Coriolis force, which deflects the westward surface currents to the left in the Southern Hemisphere. This leads to a net on-shore transport in the upper-ocean boundary layer (surface Ekman layer). The resulting convergence of surface water at the ice front locally lifts the sea surface and induces a regime of coastal downwelling. The sloping sea surface gives rise to a meridional (north-south) pressure gradient across the front, which is leads to a geostrophic current flowing westward along the shelf break. Being vertically uniform (barotropic), this current is balanced by friction in a bottom boundary layer (bottom Ekman layer), inducing a northward transport along the seabed.

In addition to the Ekman overturning sketched by Sverdrup (1953), the accumulation of lighter surface water over the continental shelf, and its depression due to the coastal

downwelling, induces a density contrast across the front. The associated pressure difference gives rise to a vertically sheared (baroclinic) component of the ASF current, which is superimposed to the barotropic flow (Nunez-Riboni and Fahrbach, 2009). A fundamental property of such baroclinic currents is their ability to become unstable for sufficiently large vertical shears (Gill, 1982). In this case small perturbations of the mean flow grow exponentially by converting available potential energy associated with horizontal density gradients into kinetic energy. This produces baroclinic eddies, vortices that circulate around isolated density anomalies, like the atmospheric cyclones and anticyclones that determine our daily weather. These eddies interact with the mean flow, causing a net transport across the front that flattens out the sloping surfaces of constant density, and counteracts the wind-driven Ekman overturning. The overturning induced by such an eddy circulation has been found to play an important role for the momentum balance and the transports across frontal currents. The most prominent example is the Antarctic Circumpolar Current, where the eddy overturning is believed to balance the Ekman driven upwelling of deep-ocean water (Marshall and Radko, 2003). A major objective of this study is to investigate the role of the eddy-driven overturning associated with the ASF for the heat supply for basal melting of ice shelves along the EWS coast.

Another coastal process that is important for the ice shelf cavity ventilation is the seasonal cycle of surface water properties, induced by the seasonal freezing and melting of sea ice. Most of the sea ice cover in the EWS melts during summer, with only small areas of multi-year ice being present along the coast (Fraser et al., 2012). During fall, when atmospheric temperatures drop far below freezing, the heat loss of the open ocean is large, causing sea ice growth. Freezing of seawater releases salt, which increases the density of the surface water and induces convective mixing. In many regions of Antarctica, this process is efficient enough to mix cold surface water throughout the entire water column, producing the dense Antarctic Bottom Water, which plays an important role in the global ocean circulation (Gill, 1973). Along the EWS coast however, such dense water masses are not observed, with the water masses over the continental shelf being usually less dense than the warmer deep-ocean water off-shore (Nicholls et al., 2009).

The sea ice growth sustains until the end of the winter, when the increased solar radiation initiates the melting season. During this period, fresh water stored in the sea ice is released to the ocean and strengthens the stratification of the coastal water column. Solar heating also warms up the surface water up to several tenths of degrees above the freezing point.

2.3 Basal Melting at the Fimbul Ice Shelf

2.3.1 Previous work at the Fimbul Ice Shelf

With an area of about 40,000 km^2, the FIS is the sixth largest Antarctic ice shelf and the largest ice shelf in Dronning Maud Land (Melvold et al., 1998), being located at the Greenwich meridian, indicated by the red square in the inset in Figure 2.5. Its geometrical configuration is typical for the ice shelves along the EWS coast, and one reason for studying the basal melting of the FIS is the availability of a rich data set of the Fimbul region (in terms of the data-density-standard in Antarctica) from earlier work.

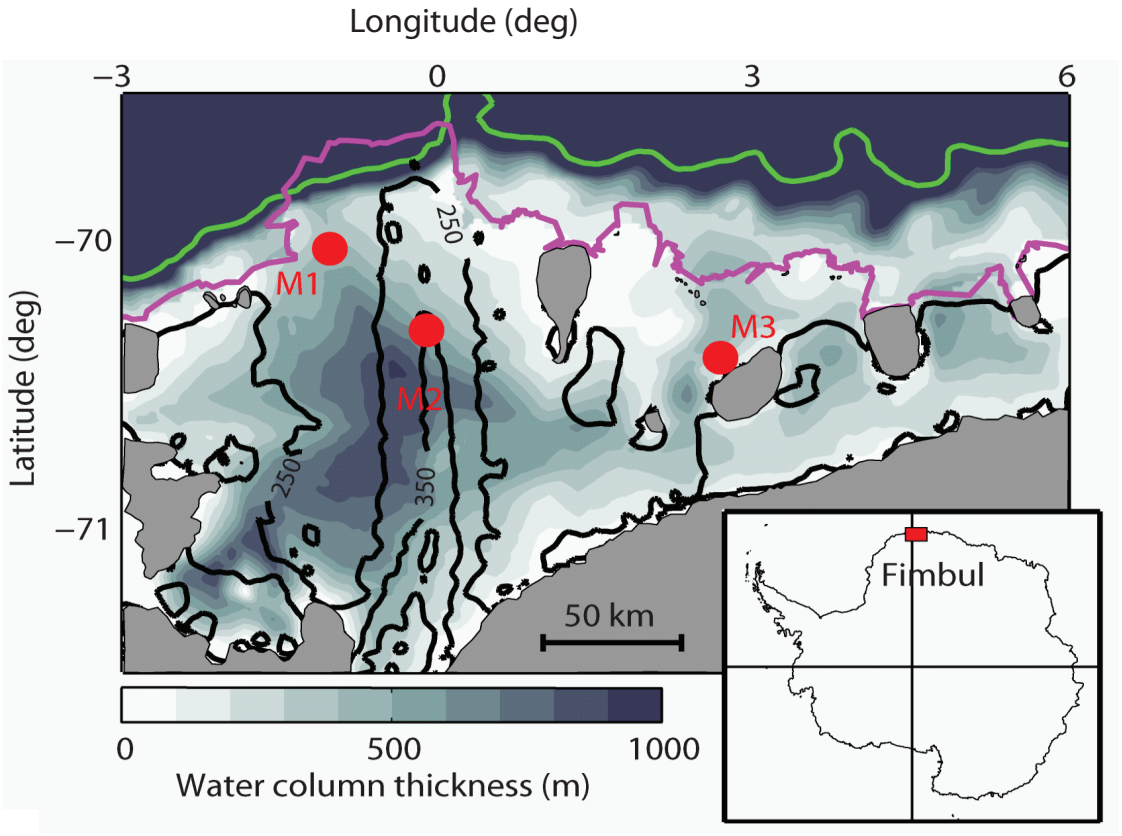

Figure 2.5: *A map of the FIS geometry. Gray shades show the thickness of the water column below the ice, which is equivalent with the bottom depth in the open ocean. The continental shelf break runs approximately along the 600 m shade, with the transition towards the deep-ocean being indicated by the green 1500 m contour. Black contours indicate the ice draft depth, with the ice front shown in magenta. Uniform gray patches indicate grounded ice. The locations of the mooring M1, M2 and M3 are shown in red.*

An intense seismic survey conducted in the austral summer 2001/02 has shed light on the geometrical configuration of the ice shelf cavity, presented by Nøst (2004). Although remote sensing based radar measurements provide a good overview of the ice thickness of most of the Antarctic ice shelves (Lythe et al., 2000), the detailed map of the sub-ice shelf bottom topography provided by the seismic data is unique in the EWS and unrivaled below most of the Antarctic ice shelves.

A map of the water column thickness and the depth of the ice shelf draft in the FIS region is shown in Figure 2.5. In the east, the ice shelf consists of a rather shallow part with uniform ice thickness of up to 300 m and a water column thickness seldom exceeding 500 m. In the central part of the FIS, a keel of much thicker ice extends along the flowline of the Jutulstraumen ice stream, that enters the ice shelf in the southernmost part of the map. Below the thick ice the ocean is much deeper, forming the central basin of ice shelf cavity. Most of the exchange between the cavity and the open ocean is believed to occur across the main sill (close to the point marked by M1) and the eastern sill (close to the point marked by M3), which are the deepest connections to the interior of the cavity. Another characteristic feature is the ice tongue of Jutulstraumen, which overhangs the shelf break and interacts directly with the coastal current, following the continental slope.

Another motivation for focusing on the FIS is that melt rates suggested by earlier modeling studies are in disagreement with those diagnosed from from satellite mass balance estimates. The models of Hellmer (2004) and Smedsrud et al. (2006) simulate the direct inflow of WDW into the cavity, causing average melt rates in the order of several meters per year. The associated basal mass loss exceeds by far the ice flux across the grounding line estimated by Rignot et al. (2008). If the models were correct, this would suggest a substantial net mass loss and thinning of the ice shelf. However, the sub-ice shelf observations based on an autonomous underwater vehicle, presented by Nicholls et al. (2006), showed no traces of the WDW inside the cavity. Also the water mass analysis of Price et al. (2008) and the ice flow modeling by Humbert (2010) suggest that basal melt rates are lower than suggested by the ocean models. Finally, the ice shelf - ocean model presented by Nicholls et al. (2008) simulated less WDW inside the FIS cavity and melt rates in the order of one meter per year, which is more consistent with the remote sensing based melting estimates.

However, none of the previous sub-ice shelf circulation models were able to sufficiently resolve the dynamic processes of the ASF, limiting their ability to study the details about the cavity exchange. Particularly little was known about the role of the eddy overturning described in Section 2.2 prior to this study. Beside the observational snapshot provided by Nicholls et al. (2006), and a set of observations through an ice rift in the southern periphery of the ice shelf cavity presented in Nicholls et al. (2008), there existed also no direct observations of the water masses and the circulation below the FIS.

2.3.2 Oceanographic Fieldwork and Data

A major achievement of the work presented in this thesis is the acquisition of a set of direct observations of the ocean circulation below the FIS. As part of the ICE–Fimbul–Top-to-Bottom project, three oceanographic moorings were deployed through the main

body of the ice shelf during a ground-based research expedition in the austral summer season 2009/2010.

The moorings M1, M2 and M3 were lowered below the ice through three hot water-drill holes at the locations indicated on the map in Figure 2.5. The moorings consisted of two Aanderraa RCM9 current meter instruments, each located close to the ice base and near the seabed, respectively. Hourly time series of horizontal current speed and direction, conductivity, temperature, and dissolved oxygen at each instrument were stored at the surface of the ice shelf. The data were retrieved during two successive revisits at yearly intervals. In addition, continuous Conductivity, Temperature, Depth-profiles (CTD-profiles) were taken through the drill holes at deployment time with a Seabird SBE49 instrument. The location of the drill holes and the vertical configurations of the moorings are shown in Table 2.1.

Table 2.1: *Coordinates of the hot water drilling sites at deployment time, and vertical configuration of the oceanographic moorings.*

mooring	location Lon / Lat	ice draft depth (m)	bottom depth (m)	upper sensor depth (m)	lower sensor depth (m)
M1	1.029 W 70.035 S	185	653	221	544
M2	0.108 W 70.316 S	345	876	369	683
M3	2.691 E 70.413 S	158	533	195	445

Another important data source utilized in this study is the set of about 2300 CTD-profiles that were collected by seven southern elephant seals (Mirounga leonina), which were captured and equipped with Satellite Relay Data Loggers on Bouvetøya (54°25'S 3°21'E) during fall 2008 (seal data[1] hereafter). Providing an eight month time series of temperature an salinity on the EWS continental shelf during Austral Winter 2008, the seal data is a unique sample of the seasonal cycle of the coastal hydrography in this sector of Antarctica. Although not directly being part of this thesis, the analysis of the seal data presented in Paper 1 had important implications for this study and set the outline for the work presented in this dissertation.

Together with two sets of ship based CTD-profiles taken along the EWS coast, being presented by Nicholls et al. (2006) and Nøst and Lothe (1997), the sub-ice shelf observations and the seal data are the main data sources for the oceanographic analysis presented in this thesis.

[1]The seal data were acquired as part of the the International Polar Year Marine Mammal Exploration of the Oceans Pole to Pole research programme (IPY MEOP). The dataset is utilized with the courtesy of Drs. Kit M. Kovacs, Martin Biuw and Christian Lydersen who were responsible for acquiring these data.

3 Results

3.1 Summary of Paper 1

Eddy overturning of the Antarctic Slope Front controls glacial melting in the eastern Weddell Sea

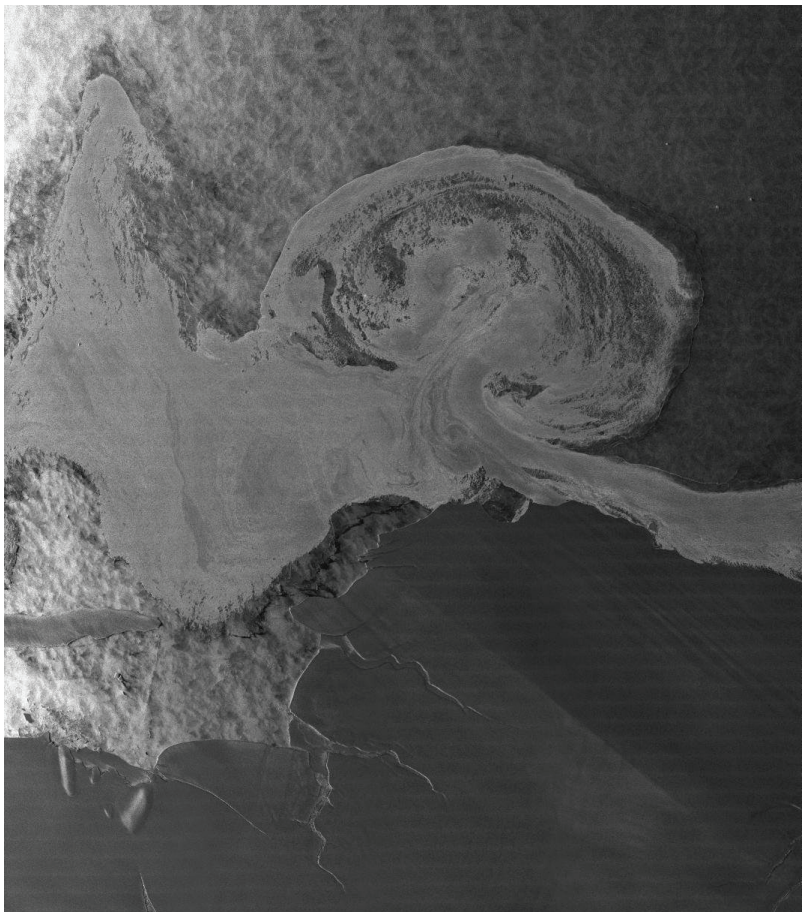

Figure 3.1: *An eddy being advected passed the FIS front as seen from space. During fall, newly forming sea ice visualizes the path of surface currents, with the eddy having a diameter between 30 to 40 kilometers. The ice shelf is seen as gray area in the lower part of the figure. The satellite images are shown with courtesy of the German Space Agency (DLR), which via AO LAN0013 TerraSAR-X provided the image to Angelika Humbert*

This paper investigates the processes controlling the water mass exchange over the continental slope in the EWS, with a particular focus on the role of the ASF eddy overturning for the on-shore transport of heat from the WDW that resides below the shelf break.

The first part of the paper presents a thorough analysis of the seal data mentioned in Section 2.3.2, and develops a conceptual model of seasonal evolution of the coastal salinity budget. This part has been developed independently from the work being presented in this thesis, and should not be regarded as a contribution to the dissertation. However, the results from this analysis have lead to the dynamical picture of the ASF presented in Section 2.2, hypothesizing the important role of the eddy overturning for the coastal momentum balance and the transport of warm water into the ice shelf cavities.

The results from the seal data analysis set the outline for the numerical modeling study, that is presented in the second part of the paper and contributes to this dissertation: A high-resolution, general ocean circulation model has been set up for an idealized ASF-continental shelf - ice shelf system, in order to explore the characteristics of the eddy overturning circulation.

The numerical code is based on the Regional Ocean Modelling System presented by Shchepetkin and McWilliams (2005) (ROMS hereafter) and was adapted by (Dinniman et al., 2003; Galton-Fenzi et al., 2012) to include a thermodynamically active ice shelf component. Being applied to a simplified periodic channel geometry, the model simulates the leading order dynamics of the ASF-circulation, capturing the interplay between the Ekman overturning and the counteracting eddy fluxes described in Section 2.2. The model shows that eddy fluxes over the continental slope act to transport a modified version of the Warm Deep Water (MWDW) originating in the ASF-thermocline onto the continental shelf, from where it may access the ice shelf cavities, thus playing an important role for the coastal heat and salt budget, and potentially contributing to basal melting along the EWS coast. This is illustrated by decomposing the simulated cross-slope transport into the respective eddy contribution and the mean flow, based on the Temporal-Residual-Mean framework presented by McDougall and McIntosh (2001). The model results are evaluated by directly comparing the simulations with a CTD-profile beneath the FIS, showing that the sub-ice shelf properties are reproduced remarkably well by the rather simple model configuration. The model results also suggest that eddy fluxes along the sloping topography may be the origin of the observed upward sloping surfaces of constant density near the seabed, which are believed to be associated with the ASF-undercurrent (Chavanne et al., 2010).

Finally, the CTD-profiles from below the FIS are presented for the first time in this paper, suggesting, together with the seal data, that the ISW in the EWS does not originate from the direct inflow of WDW below the ice shelves. This suggests the importance of the on-shore transport of sea ice - melt water in the surface Ekman layer for the coastal salinity budget, as opposed to the freshening of the continental shelf waters by large amounts of glacial melt water that was earlier proposed by Fahrbach et al. (1994).

3.2 Summary of Paper 2

Two years of oceanic observations below the Fimbul Ice Shelf, Antarctica

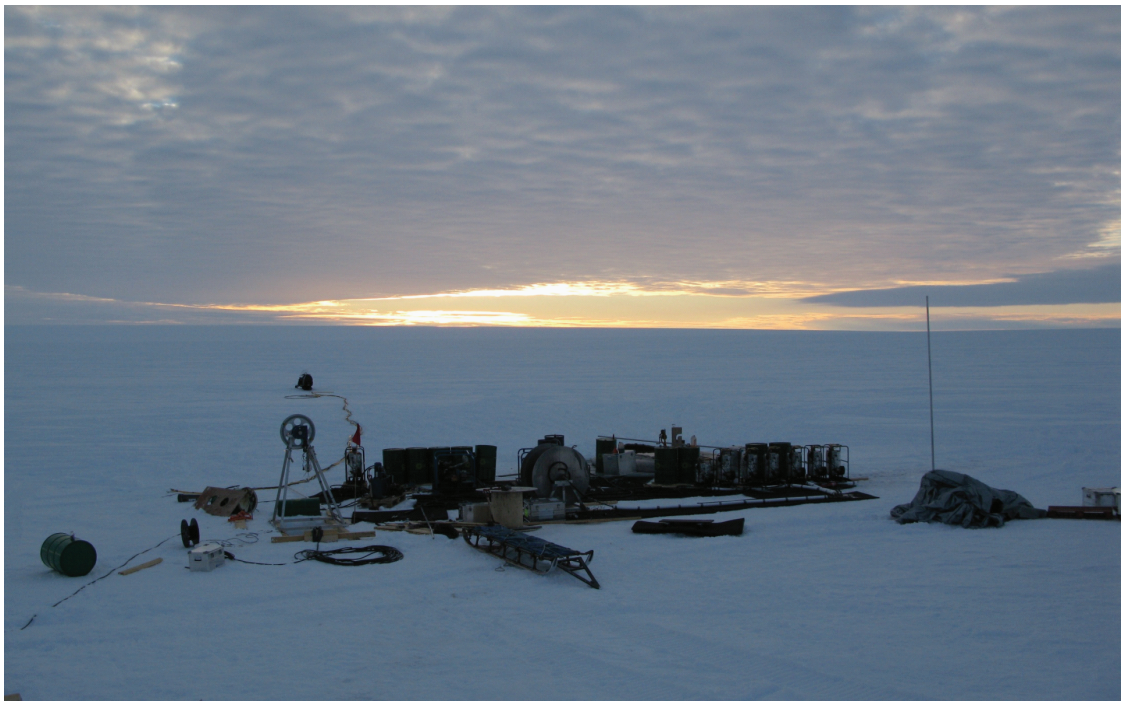

Figure 3.2: *Hot-water drilling on the Fimbul Ice Shelf. Photo: Tore Hattermann*

This paper presents the new oceanographic data, which were collected below the FIS as part of this dissertation. Apart from being a unique sample of the oceanic properties below one of the major Antarctic ice shelves, the observations have shed light on several aspects of basal melting below the FIS and the ice shelf - ocean interaction in the EWS.

One major result is that the data shows no signs of the direct access of WDW to the ice shelf cavity. The primary observation of ESW with temperatures at the surface freezing point suggests that basal melting is mainly caused by a freezing point depression-mode ice pump circulation, suggesting generally low basal mass loss below the FIS.

In addition, the data provides a detailed insight into the cavity ventilation and the exchange with the open ocean circulation. In the upper part of the water column, the data reveals a pronounced seasonal cycle, with fresh and solar heated ASW flushing parts of the ice base during late summer and fall. This confirms the presence of a mode 3-type circulation below the FIS, which enhances the melting of shallow ice due to the direct interaction of surface water with the ice base. However, the ASW is produced by sea ice melting at the surface, and its presence inside the ice shelf cavity rises the question about the dynamical process that causes the subduction of this buoyant water mass below several hundred meters of ice draft. A detailed analysis of the underlying processes causing the transport of ASW below the ice shelves in the EWS has therefore become the subject of Paper 4 in this thesis.

The observations have also shed light on the deep-ocean heat fluxes, which may cause melting in a mode-2 type circulation beneath the FIS. Although the access of warm water at depth is more constrained than suggested by the modeling studies of Hellmer (2004), Smedsrud et al. (2006), and Nicholls et al. (2008), the data shows pronounced pulses of MWDW, entering the ice shelf cavity over a three months period during late winter and spring in 2010. These pulses, which access the cavity over the main sill near the M1 mooring, are closely linked with enhanced flow speed near the seabed and strongly rotating current vectors, supporting the hypothesis of the first paper, that eddies are the reason for these deep-ocean heat fluxes.

The picture of the ice shelf cavity ventilation emerging from the observations strongly suggests that there is no simple relationship between basal melt rates and deep-ocean temperatures or continental shelf width, as it had been earlier proposed by Beckmann and Goosse (2003) or Holland et al. (2008). Instead, the data shows that basal melt rates are controlled by the complex interplay of all three modes of heat supply suggested by Jacobs et al. (1992), connecting basal melting below the FIS to both to solar forcing at the surface and to the coastal current dynamics that determine deep oean heat fluxes. This result set the outline for the modeling work presented in Paper 3 of this dissertation, which attempts to quantify the amount of melting below the FIS, and the respective contribution of the individual heat sources.

3.3 Summary of Paper 3

Modeling Basal Melting at the Fimbul Ice Shelf, Antarctica

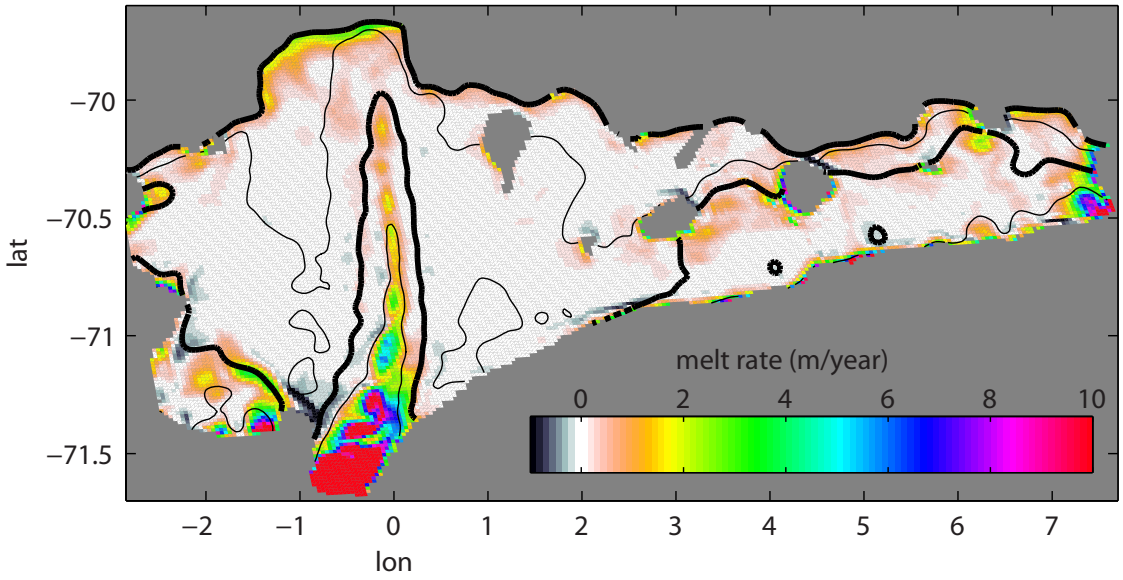

Figure 3.3: *A map of simulated melt rates below the Fimbul Ice Shelf*

Paper 3 presents the results from an eddy-resolving ice shelf - ocean general circulation model of the Fimbul region. Based on the findings in Paper 1 and Paper 2, the model is designed assessing a twofold objective, aiming to i) quantify the present basal mass loss below the FIS; and ii) to study the mechanisms that regulate the heat supply below the ice.

Being technically similar to the model presented in Paper 1, the ROMS code is applied to a realistic topography of the FIS cavity, comprising a comprehensive model forcing that allows to simulate a quasi-steady state of the ASF-current along the shelf break. For a realistic open ocean-forcing, the simulations reproduce the sub-ice shelf observations presented in Paper 2, suggesting that the model is capable to provide a good estimate of basal melt rates below the FIS. The simulated average melt rate is about 0.5 m a^{-1} at the ice base is lower than the previous model-based estimates.

In addition, the paper investigate the response of basal melting at the FIS to different climatic conditions. The study reveals that the ice shelf cavity exchange is determined by a complex interplay of processes, which is summarized in Figure 3.4. Internal dynamics of the ASF cause an opposite response of melting of deep and shallow ice to different wind stress and upper-ocean salinity. The melting of deep ice is largely determined by the depth of the ASF-thermocline relatively to the continental shelf break, which controls the access of WDW into the cavity. Melting of shallow ice in contrast is mainly controlled by the intensity of the upper-ocean circulation, which determines the shallow heat exchange across the ice front. Thereby the increased temperatures of the solar heated ASW act as an additional heat source, which causes a net increase of the shallow melting, when ASW is present in the model.

Another important finding is that varying melt rates are strongly modulated by the ice shelf geometry, and in particular the unequal distribution of deep and shallow ice below the FIS. Together with the differentiated response of the cavity exchange to coastal changes, this leads to an sharp transition between two different states of melting: In the present state of shallow melting, only small amounts of MWDW enter the cavity in eddy-like pulses and melting is dominated by low melt rates below large areas of shallow ice. This is opposed by a state of strong melting, where a rising ASF-thermocline establishes the continuous inflow of MWDW into the cavity, and a pronounced mode 2-type circulation causes high melt rates below deeper ice. The threshold for the transition between these to states is directly determined by delicate balance between the Ekman overturning and the counteracting eddy fluxes. In addition to the effect of varying surface winds, the simulations show that the buoyant surface water within the coastal water column plays an important role for this balance.

The findings in Paper 3 have finally lead to the parameterization of FIS-basal melting proposed in Section 3.5, which is reproduces the ROMS results based on a few deterministic parameters of the coastal circulation.

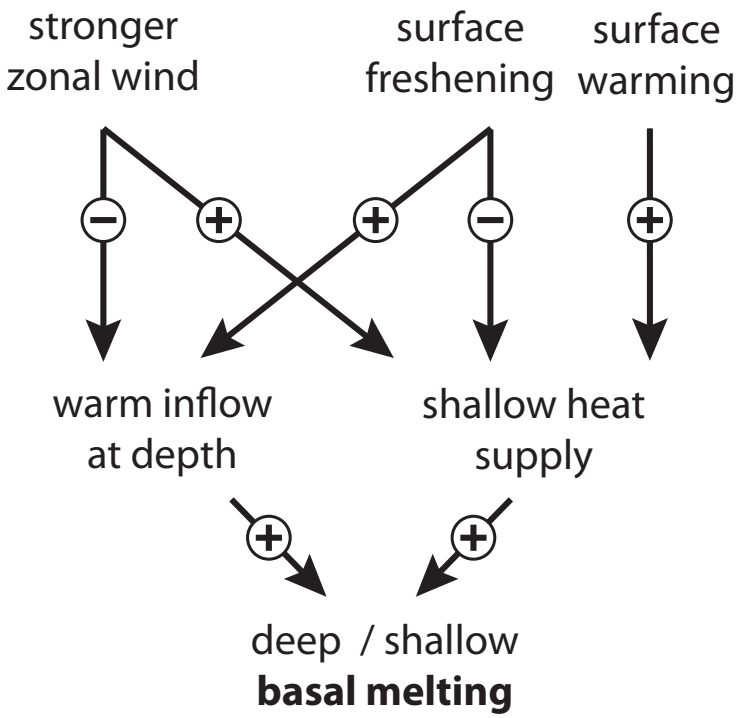

Figure 3.4: *Varying surface stress affect deep and shallow melting in opposite ways: Wind driven downwelling depresses the ASF-thermocline below the shelf break, limiting the deep melting by preventing the inflow of warm water at depth. Simultaneously, stronger winds increase shallow melting by enhancing the upper-ocean heat exchange. The dynamic effect of buoyant surface water competes the deep and shallow melting response to varying winds: Increased fresh water supply enhances the warm inflow at depth by lifting up the thermocline, while the increased upper-ocean stratification reduces shallow melting, by decoupling the coastal current from the cavity circulation. In addition, spreading of ASW below the ice also acts as a direct source of sensible heat for shallow melting.*

3.4 Summary of Paper 4

Wind-driven spreading of freshwater beneath the ice shelves in the Eastern Weddell Sea

Figure 3.5: *Sensor equipped Southern Ocean Elephant Seal ready to collect oceanographic data. Photo: Martin Biuw*

This paper is concerned with the processes causing the access of buoyant surface water below the ice shelves in the EWS. The motivation for this study arose from the observation of ASW below the FIS, which is reported in Paper 2.

The paper proposes that the subduction of ASW below ice draft is primarily caused by the wind-driven accumulation and downwelling of surface water along the ice front. The validity of this hypothesis is explored in three different ways: i) A detailed analysis of the seal-data in combination with sea ice thickness maps from Worby et al. (2008) reveals that local sea ice melting may not explain the observed seasonal freshening of the continental shelf water masses. Instead, the data shows that the accumulation of fresh water, being produced by melting off shore, is a feasible explanation of the observed seasonal cycle; ii) An analytical model of the coastal momentum balance is proposed, showing that the Ekman overturning may cause the sufficient subduction of buoyant surface water below the ice shelf depth, given a realistic parameter range; iii) The analytical model is supported by idealized numerical simulations based on the simplified ROMS model setup presented in Paper 1. The simulations confirm the linear relationship between the downwelling depth of the ASW and the applied stress at the ocean surface. The comparison of the three-dimensional simulations with an eddy-free two-dimensional setup also demonstrates the crucial contribution of the eddies to the coastal momentum balance, which will not reach the quasi-steady equilibrium when eddies are excluded.

This paper is placed at last in the list of papers, because, although many of the ideas presented in Paper 4 arose during the work presented in this Chapter, some of the work presented in Paper 4 should not be regarded as part of this dissertation. In particular the development of the analytical model, the technical handling of the seal data analysis, and the adaptation of the ROMS model for the scope of the paper, as well as the production of the figures, and most of the writing were carried out by Qin Zhou, and should be regarded independently from this thesis. However, the scientific objective and the red thread of the paper are a common result of fruitful discussion, which deserves to be mentioned here, last but not least, also to complete of the dynamical picture of the ASF-circulation presented in this dissertation.

3.5 Basal Melting Parameterization for the Fimbul Ice Shelf

3.5.1 The Modified Plume Model

Paper 3 identifies two important parameters that control melting below the FIS: (i) the thermocline depth within the ASF determines the amount of MWDW that enters ice shelf cavity, controlling the deep melting; and (ii) the strength of wind induced surface currents determines the efficiency of the upper-ocean heat supply, controlling the shallow melting. Furthermore, the analysis of the melting distribution has shown that the contribution of melting at different depths is largely determined by the geometrical configuration of the ice shelf.

This section derives a simple parameterization for melting below the FIS, by incorporating these characteristic features of the cavity circulation into to the plume model presented in Section 2.1.3.

Jenkins (1991) originally considers a uniform width of the plume path along the ice base. However, in reality one would expect the presence of several, dynamically independent plumes at different locations below the ice shelf. The analysis in Paper 3 shows that the uneven distribution of ice shelf area strongly affects the contribution of melting at different depths. In order to take this effect into account, the model equations are rewritten, introducing a variable width w of the plume. Using the same notation as in section 2.1.3, this yields the following form of the equations for conservation of mass, momentum, heat and salt, which were presented in equation 2.1 to equation 2.4:

$$\frac{d\left(UDw\right)}{dx} = w\left(\dot{e}+\dot{m}\right) \tag{3.1}$$

$$\frac{d\left(U^2Dw\right)}{dx} = -Dw\Delta\rho\; g\sin\Theta - KU^2w \tag{3.2}$$

$$\frac{d\left(TUDw\right)}{dx} = w\left[T_{SW}\dot{e}+T\dot{m}+\left(T_0-T\right)\gamma_T\right] \tag{3.3}$$

$$\frac{d\left(SUDw\right)}{dx} = w\left[S_{SW}\dot{e}+S\dot{m}+\left(S_0-S\right)\gamma_S\right] \tag{3.4}$$

Here, UDw is the total volume flux through a cross section of the plume. The melt ($\dot{m}$) and entrainment ($\dot{e}$) rates are given per area, and need to be multiplied with the plume width at respective depth, in order to obtain the total mass flux across the upper and lower boundary of the plume layer. w describes the total ice shelf area as a function of depth, and it is assumed that the plume at all depths extends over the entire ice base. Thereby, we also neglect any motion perpendicular to the flow direction of the plume associated with changes of the plume width.

In reality, ISW plumes tend to rise rather localized along a flow lines of steeply sloping ice, and the assumption of a single plume that spans the entire ice shelf is rather unphysical. However, the modification improves the original model by incorporating an important

geometrical effect, that appears to significantly alter the melting distribution below the FIS. In a uniform plume, melting of deep ice produces a relatively large amount of buoyant ISW. This accelerates the plume at shallower depth and increases melting along the entire plume path. Below the FIS, much of the total melting is caused by weak melting of large areas of shallow ice, and the amount of ISW that is produced at the small area of very deep ice affects only a minor fraction of the shallow ice base. How this is included in the plume model becomes evident, when rewriting equation (1) to (4) as differential equations for the individual variables D, U, T, and S. For momentum, heat, and salt, the equations remain unchanged from the case with uniform width. But rewriting the thickness equation yields

$$\frac{dD}{dx} = \frac{2\,(\dot{e} + \dot{m})}{U} + \frac{D\Delta\rho\; g \sin\Theta}{U^2} + K - \frac{dw}{dx}\frac{D}{w}, \tag{3.5}$$

with the last term on the right hand side being related to the variable plume width.

When the ice shelf widens at shallower depth, the plume will become thinner as it rises along the ice base, in order to conserve its total mass. A thinner plume comprises less thermal inertia and its properties are more easily affected by entrainment of the ambient water. In this way the modification better represents the geometrical configuration of the FIS, where only a small fraction of shallow ice base is directly affected by deeply originating plumes, and most of the shallow melting is primarily controlled by the upper-ocean forcing.

Also the geometry of the path of the plume along the ice base needs to be specified. The flow speed of the gravity-driven plume generally depends on the slope of the ice. Here, a characteristic ice shelf profile is used, derived from the horizontally averaged slope as a function of ice shelf depth. The shape of this profile is shown in by the blue curve in Figure 3.7a, together with the distribution of ice shelf area as a function of ice shelf depth (red curve). The model also allows the evolution of multiple plumes that originate when the previous plume detaches from the ice base. In this way, it is assured that always the entire ice shelf area contributes to the total melting estimate.

3.5.2 Input Parameters

Next, an ambient ocean forcing is constructed that includes the leading processes controlling basal melting at the FIS. The original formulation of the plume neglects the fluid motion in the ambient layer (Jenkins, 1991). Here, the effect of the wind-induced sub-ice shelf circulation on the heat supply for shallow melting is included, by assuming that upper-ocean currents generally enhance turbulent mixing across the vertical boundaries of the plume. A similar modification has earlier been used by Smedsrud and Jenkins (2004) to include the effect of tides on basal melting. With an ambient ocean velocity U_a, the parameterization for the entrainment (eqn. 2.5) of ambient water into the plume is then given by

$$\dot{e} = E_0\,(U + U_a)\sin\Theta, \tag{3.6}$$

and the expressions for the transfer coefficients of heat and salt across the ice - ocean boundary layer become

$$\gamma_T = \gamma_{0_T} (U + U_a), \text{ and } \gamma_S = \gamma_{0_S} (U + U_a), \tag{3.7}$$

respectively. Here γ_{0_T}, and γ_{0_S} correspond to the transfer coefficients of the unmodified version of the model being described by Jenkins (1991).

Furthermore, the effect of the interaction of the thermocline with the shelf break, which controls the deep melting, is incorporated. The relationship between the thermocline depth z_{tc} and the deep-ocean heat supply is represented by an ambient ocean temperature profile $T_a(z)$, of the following form:

$$T_a(z) = \begin{cases} T_l + (T_u - T_l) \left(1 + e^{-2\Delta_z (z - z_{tc})}\right)^{-1} & \text{if } z \leq z_{sill}, \\ T_a(z_{sill}) & \text{if } z > z_{sill} \end{cases} \tag{3.8}$$

Here, $T_u = -1.9\,^{\circ}\text{C}$, and $T_l = 0.5\,^{\circ}\text{C}$ are the respective deep and upper-ocean temperatures, with $\Delta_z = 50$ m being the thickness of the MWDW layer at the over the continental shelf. The position of the thermocline relative to the main sill depth $z_{sill} = 550$ m at the FIS determines if the WDW reaches the deep ice, with a smooth transition of deep-ocean temperatures inside the cavity, when the thermocline is located close to the sill.

3.5.3 Forcing based on ROMS Simulations

The parameterization is evaluated, by reproducing the melt rates that were obtained from the ROMS simulations in Paper 3.

The characteristic response of melting below the FIS as discussed in Paper 3 is summarized in Figure 3.6. The upper two panels compare the melting of shallow and deep ice (obtained by integrating the area below the curves in Figure 7c of Paper 3) for the different model experiments. Each panel shows the total amount of melting as a function of wind forcing (colored curves), together with the contribution of melting below 300 m depth (colored patches Figure 3.6a) and melting shallower than 300 m depth (colored patches Figure 3.6b). The shallow melting increases linearly with increasing surface stress and dominates the total melting response in the experiments with stronger winds. The deep melting, in contrast, shows only little variation for stronger winds. For weaker winds, however, melting at depth increases drastically and dominates the total melting response. The different colors in Figure 3.6 correspond to the different hydrographic scenarios applied for restoring of upper-ocean properties in the model forcing: An annual climatology (blue); a constant winter scenario (grey); and a constant summer scenario (yellow).

The modified plume model is now used to reproduce the simulated basal melt rates as a function of varying wind strength in different hydrographic scenarios. Thereby, the forcing parameters U_a and z_{tc} for the melting parameterization are directly obtained from the ROMS results.

The average depth of the thermocline near the main sill as diagnosed from the different experiments is presented in Figure 3.6c. Comparing these results with the deep melting

shown in Figure 3.6a clearly shows that the melting of deep ice drastically increase when the thermocline rises above the sill depth (indicated by the horizontal line). The diagnosed thermocline depth is directly used to specify the deep-ocean forcing z_{tc} in the plume model.

The dynamic forcing for each experiment in the plume model is specified by a constant velocity U_a in the upper 300 m of the ambient ocean and no currents below that depth. The average velocity at the ocean surface beneath the shallow ice is diagnosed from the ROMS results, being shown in Figure 3.6c. As discussed in Paper 3, for moderate and strong winds, the changes in shallow melting relate directly to the current strength below the ice. For weak winds however, the large amounts of buoyant ISW ascending along the ice base dominate the flow field and the relationship between the shallow melting an the upper-ocean currents breaks down. In order to exclude this effect of the internal circulation dynamics from the forcing, the applied upper-ocean velocity is prescribed as a linear function of surface stress, derived from the three strongest wind forcings for each hydrographic scenario shown in Figure 3.6c.

In the constant winter scenario, the ambient upper-ocean temperature corresponds to the surface freezing point. In order to represent the additional heat provided the presence of the ASW in the annual and summer scenario, temperatures in the upper 200 m of the ambient ocean is increased to -1.8 °C, and -1.7 °C respectively, with a linear transition towards the deep-ocean temperature between 200 m and 300 m. This is a reasonable representation of the average upper-ocean temperatures outside the cavity in the different scenarios of the ROMS simulations. The prescribed salinity of the ambient ocean also resembles the ROMS results, but appears to be of minor importance for the melting estimated by the plume model. Ambient ocean temperature and velocity profiles of the experiments corresponding to the six ROMS simulations with annual forcing, and are shown in Figure 3.7b and c.

3.5.4 Parameterized Melting Results

The total melting together with the respective contribution of the deep and shallow ice obtained from the ROMS simulations (upper column) as well as based on the modified plume model (lower column) are shown in Figure 3.6. The similarity between the results of the simple parameterization with the melt rates based on the three-dimensional simulation of the complex ASF-system is overwhelming. The plume-model convincingly reproduces sensitivity of the deep and shallow melting to varying wind stress, with melting being generally in the same range as in the ROMS simulations. The thermocline depth regulates the deep melting, with a drastic increase of melting, once the WDW rises above the sill. Also the balance between the two counteracting effects of ASW on the shallow heat supply is captured well, with the shallow melting being largest in the constant summer scenario, although upper-ocean currents are largest in the constant winter scenario.

The most prominent difference between the plume-model and the ROMS results is the stronger melting of shallow ice in the plume model. The shallow melting is generally very sensitive to the upper-ocean temperatures, and here, the ambient ocean temperature profile is prescribed to represent the temperature distribution of the upper-ocean outside

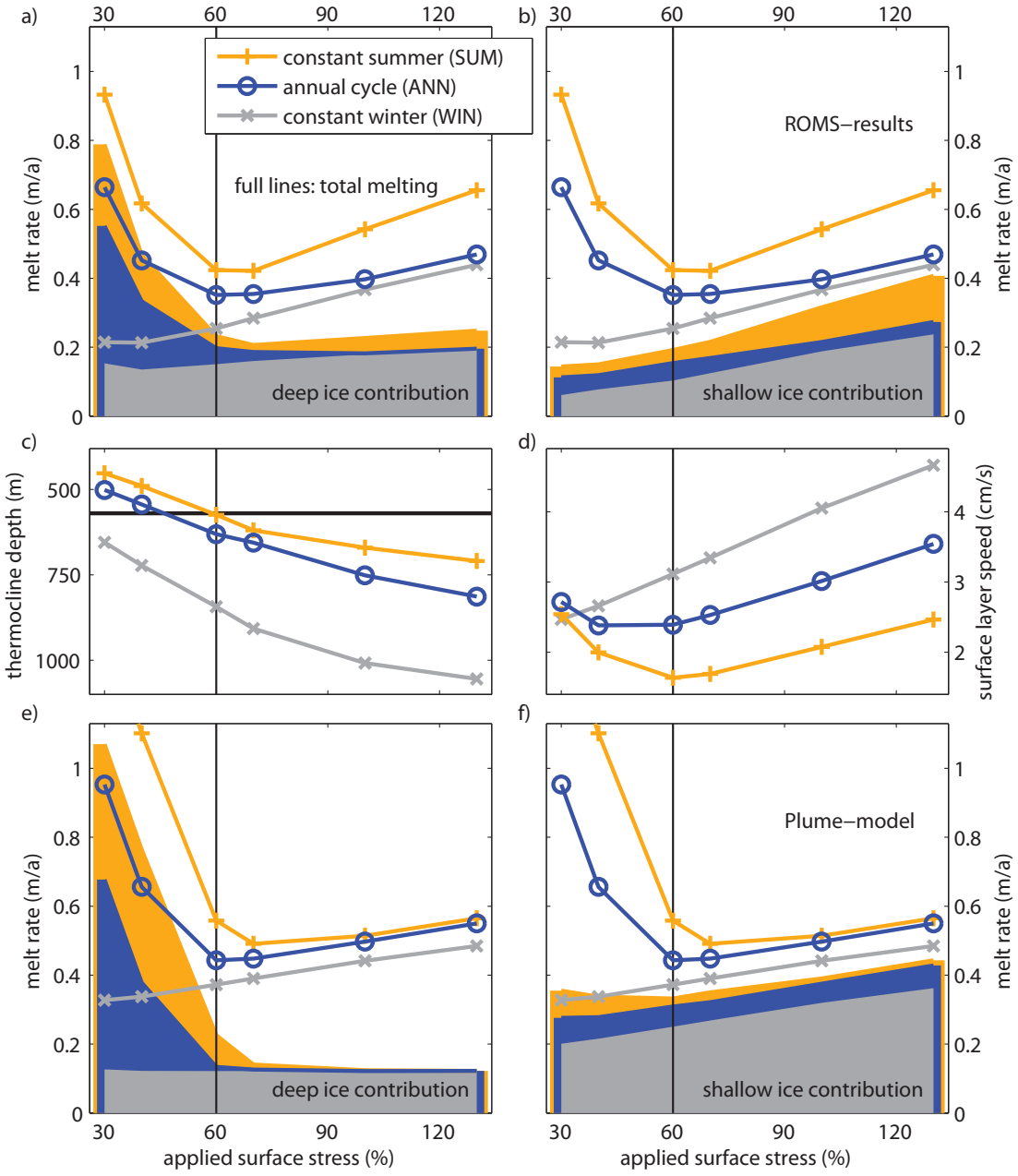

Figure 3.6: *Simulated basal melting as obtained with the three-dimensional ROMS simulations (upper row) compared to the results of the plume model (lower row). The net basal melting of deep ice below 300 m depth and shallow ice between 140 m and 300 m depth as a function of wind forcing given for the different hydrographic scenarios is shown by the colored patches in Figure 3.6a/e and b/f. The full lines are equal in both panels, showing the net mass loss of the entire FIS. Figure 3.6c shows the depth of the ASF-thermocline in the main sill area, with the sill depth being indicated by the black horizontal line. Figure 3.6d shows the average current speed in the ocean surface layer below the shallow ice. The maximum net melting around 1.4 ma^{-1} for the constant summer scenario in the plume model is not shown, in order to preserve a consistent axis scaling. The transition from the weak into the strong melting state, when the thermocline rises above the sill depth is indicated by the vertical lines in all panels.*

the ice shelf cavity. A more detailed analysis of the ROMS results shows that upper-ocean temperatures in parts of the ice shelf cavity are slightly lower than the surface freezing point, because some of the ISW is recirculated within the cavity. This possibly explains the stronger melting in the plume model that does not take this effect into account.

The good agreement between the parameterization and the ROMS results has two important implications: (i) the proper response to varying forcing confirms that Paper 3 indeed isolated the main mechanisms that control basal melting below the FIS; and (ii) the fact, that this simple parameterization of melting along a one-dimensional flowline satisfyingly reproduces the simulated melt rates, indicates that the details of the cavity circulation are of minor importance for the heat transport towards the ice. Instead, it is found that the vertical distribution of ice shelf area is generic parameter that affects the plume dynamics and needs to be considered when estimating basal melting.

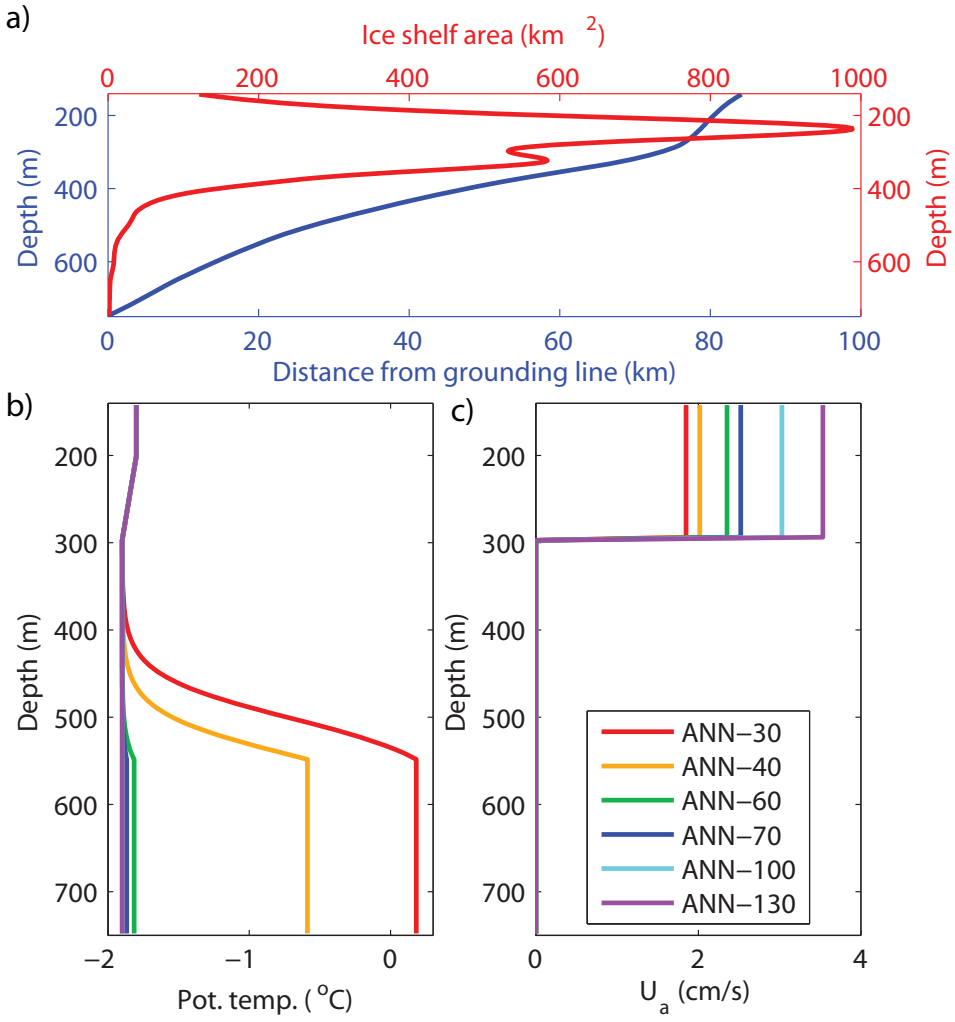

Figure 3.7: *Ice shelf geometry and ambient ocean forcing for the plume model, showing the profile of the plume path (lower and left axes in Figure 3.7a) together with the distribution of ice shelf area as a function of depth (upper and right axes in Figure 3.7a), as well as profiles of the ambient ocean temperature (Figure 3.7b) and velocity (Figure 3.7c) for the experiments in the scenario with the annual hydrographic forcing.*

4 Concluding Remarks

In this thesis the ice shelf - ocean interaction in the Eastern Weddell Sea has been explored with particular focus on basal melting at the Fimbul Ice Shelf. The presented work contributes to the overall assessment of the mass balance of the Antarctic ice sheet, by providing an improved understanding of the coastal dynamics that control the oceanic heat supply for basal ice shelf melting along the coast of Dronning Maud Land.

A major contribution of this work is the analysis of the heat sources for basal melting below the FIS, based on a unique set of direct oceanic observations within the ice shelf cavity. The thesis also presents the first eddy-resolving simulations of the Antarctic Slope Front - continental shelf - ice shelf system in the EWS region, providing an improved estimate of basal melt rates below the FIS, as well as a detailed study of the coastal processes controlling the ice shelf - ocean heat exchange.

The picture of the processes and water masses controlling basal melting along the EWS coast arising from this study is illustrated in Figure 4.1. The major conclusions are as follows:

- Water mass properties on the continental shelf and beneath the ice shelves in the EWS are determined by the balance between two opposite overturning circulations, caused by the Ekman-driven coastal downwelling of surface waters, and the counteracting eddy fluxes associated with the horizontal density contrast of the Antarctic Slope Front. A proper representation of oceanic mesoscale eddy processes is thus a crucial requirement for climate models, in order to quantify basal melting in this sector of Antarctica.

- Both observations and eddy-resolving simulations show that the access of Warm Deep Water below the Fimbul Ice Shelf is much more constrained than suggested by previous ocean models, causing substantially lower melt rates than earlier suggested. This is consistent with satellite-based mass balance estimates, and implies that the FIS is currently not subject to rapid mass loss or thinning due to basal melting.

- The model results suggest a sharp transition between two distinct states of basal melting below the FIS, which is directly controlled by the depth of the ASF-thermocline relative to the shelf break. In the present state of shallow melting, the total basal mass loss is dominated by low melt rates below large areas of shallow ice, which is mainly regulated by the upper-ocean circulation. This is opposed by the state of

deep melting, where the continuous inflow of warm water at depth causes high melt rates below deeper ice, once the thermocline rises above the shelf break depth.

- In addition to the surface wind forcing, a central role for melting below the FIS is found to be played by the Antarctic Surface Water. The presence of this buoyant and solar heated water mass enhances the shallow melting due to its additional heat supply, and alters the deep-ocean heat supply by affecting the coastal momentum balance. Also the geometrical configuration of the ice shelf, in particular the unequal distribution of shallow and deep ice strongly modulates the response of total melting to oceanic changes. However, the capability of one-dimensional plume model to reproduce the ROMS results, demonstrates that the melt rates below the FIS may be parameterized based on only a few deterministic parameters of the coastal circulation, appearing to be relatively independent of the details of the cavity circulation.

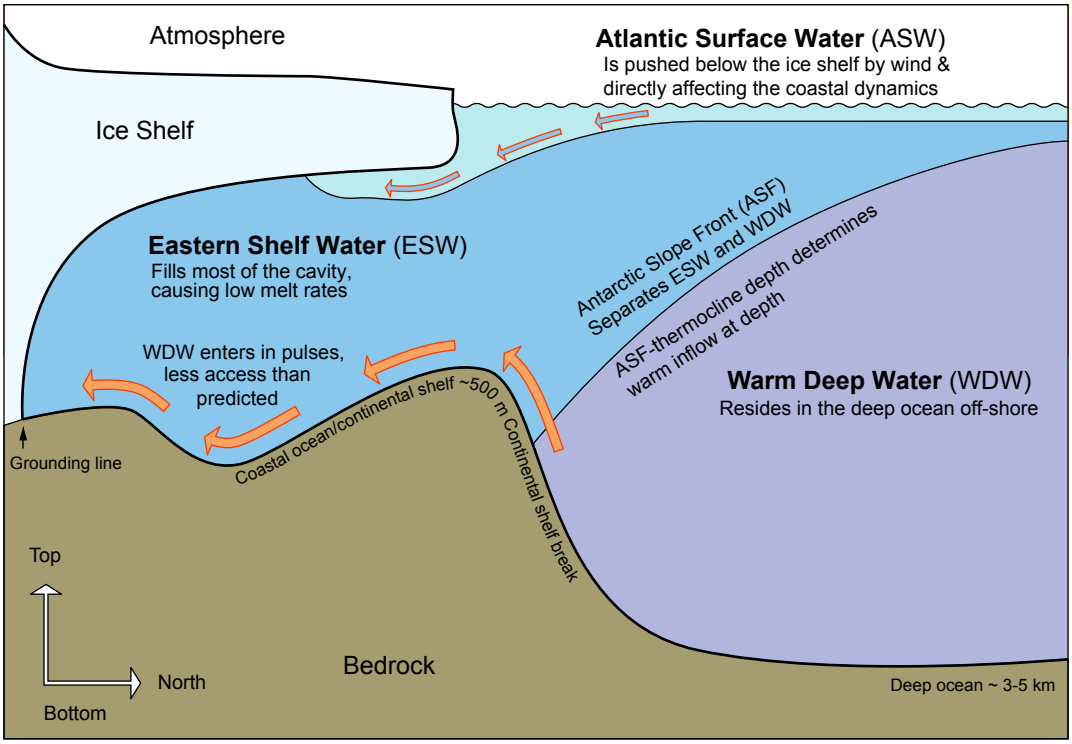

Figure 4.1: *A schematic illustration of the water masses and processes controlling basal melting along the Eastern Weddell Sea coast. Design: Audun Igesund, Norwegian Polar Institute.*

The presented work also identifies several objectives which need to be addressed in future work in order to estimate basal melting in the EWS. A major source of uncertainty for assessing ice shelf cavity ventilation is the effect of sea ice on the wind forcing. The

melting of both the shallow ice and the deep ice is directly affected by changes in ocean surface stress, and drift ice may either increase or decrease the transfer of momentum from the atmosphere (Lüpkes and Birnbaum, 2005). Another issue highlighted by the model results is the further exploration of the effect of buoyant summer water on the coastal circulation, and in particular the role of this water mass in determining the seasonal cycle of the deep-ocean heat fluxes beneath the ice. The modeling results in this thesis have also shown the important role of bottom topography for regulating the ice shelf cavity exchange. However, beneath most of the Antarctic ice shelves, the bathymetry is presently poorly known, with ocean models often relying on best-guess interpolated estimates being insufficiently constrained by observations.

Previous studies have highlighted further aspects of the ice shelf - ocean interaction in the EWS, which were not comprehensively covered in this thesis: Galton-Fenzi et al. (2012) show that the effects of freezing below ice shelves may have broader effects on the ice shelf cavity circulation; Nicholls et al. (2008) find that tidal mixing within the ice shelf cavity may cause a significant increase of melting below the FIS; and Chavanne et al. (2010) suggested that coastally trapped waves may lead to deep-ocean heat transport onto the EWS coast the continental shelf. Although the results of this study suggest other processes to be the main controls for basal melting in the EWS, the details of these processes have not been addressed properly in this study and will require further attention in future work.

Bibliography

Beckmann, A., Goosse, H., 2003. A parameterization of ice shelf-ocean interaction for climate models. Ocean Model. 5, 157–170.

Chavanne, C. P., Heywood, K. J., Nicholls, K. W., Fer, I., 2010. Observations of the Antarctic slope undercurrent in the southeastern Weddell Sea. Geophys. Res. Lett.. 37 (L13601), doi:10.1029/2010GL043603.

Dinniman, M. S., Klinck, J. M., Smith Jr., W. O., 2003. Cross-shelf exchange in a model of the Ross Sea circulation and biogeochemistry. Deep-Sea Res. Part II 50 (22–26), 3103–3120.

Dupont, T. K., Alley, R. B., 2005. Assessment of the importance of ice-shelf buttressing to ice-sheet flow. Geophys. Res. Lett. 32 (4), L04503.

Fahrbach, E., Peterson, R., Rohardt, G., Schlosser, P., Bayer, R., 1994. Suppression of bottom water formation in the southeastern Weddell sea. Deep-Sea Res. Part I 41 (2), 389–411.

Fraser, A. D., Massom, R. A., Michael, K. J., Galton-Fenzi, B. K., Lieser, J. L., 2012. East Antarctic Landfast Sea Ice Distribution and Variability, 2000–08. J. Climate 25 (4), 1137–1156.

Gade, H., 1979. Melting of ice in sea water: a primitive model with application to the Antarctic ice shelf and ice bergs. J. Phys. Oceanogr. 9, 189–198.

Galton-Fenzi, B., 2009. Modelling Ice-Shelf/Ocean Interaction. Ph.D. thesis, University of Tasmania.

Galton-Fenzi, B. K., Hunter, J. R., Coleman, R., Marsland, S. J., Warner, R. C., 2012. Modeling the basal melting and marine ice accretion of the Amery Ice Shelf. J. Geophys. Res. 117 (C9), C09031.

Gill, A. E., 1973. Circulation and bottom water production in the Weddell Sea. Deep-Sea Res. 20, 111–140.

Gill, A. E., 1982. Atmosphere-Ocean Dynamics, 1st Edition. Academic Press.

Hellmer, H. H., 2004. Impact of Antarctic ice shelf basal melting on sea ice and deep ocean properites. Geophys. Res. Lett.. 31 (L10307), doi:10.1029/2004GL019506.

Hellmer, H. H., Kauker, F., Timmermann, R., Determann, J., Rae, J., 2012. Twenty-first-century warming of a large Antarctic ice-shelf cavity by a redirected coastal current. Nature 485 (7397), 225–228.

Hellmer, H. H., Olbers, D. J., 1989. A two-dimensional model for the thermohaline circulation under an ice shelf. Antarct. Sci. 1 (04), 325–336.

Heywood, K. J., Locarnini, R. A., Frew, R. D., Dennis, P. F., King, B. A., 1998. Transport and water masses of the Antarctic Slope Front system in the eastern Weddell Sea. In: Jacobs, S. S., Weiss, R. F. (Eds.), Ocean, ice and atmosphere: Interactions at the Antarctic continental margin. Vol. 75 of Antarct. Res. Ser. American Geophysical Union, pp. 203–214.

Holland, P. R., Jenkins, A., Holland, D. M., 2008. The Response of Ice Shelf Basal Melting to Variations in Ocean Temperature. J. Climate 21 (11), 2558–2572.

Humbert, A., 2010. The temperature regime of Fimbulisen, Antarctica. Ann. Glaciol. 51 (55), 56–64.

Jacobs, S. S., Hellmer, H. H., Doake, C. S. M., Jenkins, A., Frolich, R. M., 1992. Melting of ice shelves and the mass balance of Antarctica 38, 375–387.

Jacobs, S. S., Jenkins, A., Giulivi, C. F., Dutrieux, P., 2011. Stronger ocean circulation and increased melting under Pine Island glacier ice shelf. Nat. Geosci. 4 (8), 519–523.

Jenkins, A., 1991. A one-dimensional model of ice shelf ocean interaction. J. Geophys. Res.. 96, 20671–20677.

Jenkins, A., 2010. ACDC2010: Ice Sheet - Ocean Interactions; Core Lecture 3A: Ice Shelf/Ocean Processes at the Boundary. Lecture Notes.

Joughin, I., Alley, R. B., Jul. 2011. Stability of the West Antarctic ice sheet in a warming world. Nat. Geosci. 4 (8), 506–513.

Lewis, E. L., Perkin, R. G., 1986. Ice pumps and their rates. J. Geophys. Res.. 91 (C10), 11756–11762.

Lüpkes, C., Birnbaum, G., 2005. Surface drag in the Arctic marginal sea-ice zone: A comparison of different parameterization concepts. Bound.-Layer Met. 117, 179–211.

Lythe, M., Vaughan, D. G., the BEDMAP Consortium, 2000. Bedmap - bed topography of the antarctic. 1:10,000,000 scale map. British Antarctic Survey (Misc) 9, ().

Marshall, J., Radko, T., 2003. Residual-mean solutions for the Antarctic Circumpolar Current and its associated overturning circulation. J. Phys. Oceanogr. 33 (11), 2341–2354.

McDougall, T. J., McIntosh, P. C., 2001. The temporal-residual-mean velocity. Part II: Isopycnal interpretation and the tracer and momentum equations. J. Phys. Oceanogr. 31, 1222–1246.

Melvold, K., Hagen, J. O., Pinglot, J. F., Gundestrup, N., 1998. Large spatial variation in accumulation rate in Jutulstraumen ice stream, Dronning Maud Land, Antarctica. Ann. Glaciol. (9), 231–238.

Nicholls, K., 1997. Predicted reduction in basal melt rates of an Antarctic ice shelf in a warmer climate. Nature 388, 460–462.

Nicholls, K. W., Abrahamsen, E. P., Buck, J. J., Dodd, P. A., Goldblatt, C., Griffiths, G., Heywood, K. J., Hughes, N. E., Kaletzky, A., Lane-Serff, G. F., McPhail, S. D., Millard, N. W., Oliver, K. I. C., Perrett, J., Price, M. R., Pudsey, C. J., Saw, K., Stansfield, K., Stott, M. J., Wadhams, P., Webb, A. T., Wilkinson, J. P., 2006. Measurements beneath an Antarctic ice shelf using an autonomous underwater vehicle. Geophys. Res. Lett.. 33 (L08612), doi:10.1029/2006GL025998.

Nicholls, K. W., Abrahamsen, E. P., Heywood, K. J., Stansfield, K., Østerhus, S., 2008. High-latitude oceanography using autosub autonomous underwater vehicle. Limnol. Oceanogr. 53 (5), 2309–2320.

Nicholls, K. W., Østerhus, S., Makinson, K., Gammelsrød, T., Fahrbach, E., 2009. Ice-ocean processes over the continental shelf of the southern Weddell Sea, Antarctica: A review. Rev. Geophys. 47, 23 PP.

Nøst, O. A., 2004. Measurements of ice thickness and seabed topography under the Fimbul Ice Shelf, Dronning Maud Land, Antarctica. J. Geophys. Res.. 109, C10010, doi:10.1029/2004JC002277.

Nøst, O. A., Lothe, T., 1997. The Antarctic Coastal Current – Physical Oceanographic results from NARE 1996/97. In: Winther, J. G. (Ed.), Norsk Polarinstitutt Meddelelser. Vol. 148. Norsk Polarinstitutt, pp. 51–57.

Nunez-Riboni, I., Fahrbach, E., 2009. Seasonal variability of the Antarctic Coastal Current and its driving mechanisms in the Weddell Sea. Deep-Sea Res. Part I 56, 1927–1941.

Pollard, D., DeConto, R. M., 2009. Modelling West Antarctic ice sheet growth and collapse through the past five million years. Nature 458, doi:10.1038/nature07809.

Price, M. R., Heywood, K. J., Nicholls, K. W., 2008. Ice-shelf - Ocean interactions at Fimbul Ice Shelf, Antarctica from oxygen isotope ratio measurements. Ocean Sci. 4, 89–98.

Pritchard, H. D., Ligtenberg, S. R. M., Fricker, H. A., Vaughan, D. G., Broeke, M. R. v. d., Padman, L., 2012. Antarctic ice-sheet loss driven by basal melting of ice shelves. Nature 484 (7395), 502–505.

Rignot, E., Bamber, J. L., van den Broeke, M. R., Davis, C., Li, Y., van de Berg, W. J., van Meijgaard, E., Jan. 2008. Recent Antarctic ice mass loss from radar-interferometry and regional climate-modelling. Nat. Geosci. 1 (2), 106–110.

Rintoul, S. R., Hughes, C., Olbers, D., 2001. The Antarctic Circumpolar Current System. Vol. 77 of International Geophysics Series. Academic Press, Ch. 4.6 Ocean Circulation and Climate, pp. 271–302.

Scambos, T., Hulbe, C., Fahnestock, M., Bohlander, J., 2000. The link beween climate warming and break-up of ice shelves in the Antarctic Peninsula. J. Glaciol 46, 516–530.

Scambos, T. A., Bohlander, J. A., Shuman, C. A., Skvarca, P., 2004. Glacier acceleration and thinning after ice shelf collapse in the Larsen B embayment, Antarctica. Geophys. Res. Lett.

Shchepetkin, A. F., McWilliams, J. C., 2005. The Regional Ocean Modeling System (ROMS): A split-explicit, free-surface, topography-following coordinates ocean model. Ocean Model. 9, 347–404.

Smedsrud, L. H., Jenkins, A., 2004. Frazil ice formation in an ice shelf water plume. J. Geophys. Res. 109, C03025.

Smedsrud, L. H., Jenkins, A., Holland, D. M., Nøst, O. A., 2006. Modeling ocean processes below Fimbulisen, Antarctica. J. Geophys. Res.. 111 (C01007), doi:10.1029/2005JC002915.

Solomon, S., Qin, D., Manning, M., Chen, Z., Marquis, M., Averyt, K. B., Tignor, M., L.Miller, H. (Eds.), 2007. IPCC, 2007: Climate Change 2007: The Physical Science Basis. Contribution of Working Group I to the Fourth Assessment Report of the Intergovernmental Panel on Climate Change. Cambridge University Press, Cambridge, United Kingdom and New York, NY, USA.

Sverdrup, H. U., 1953. The currents off the coast of Queen Maud Land. Norsk Geografisk Tidsskrift 14, 239–249.

Thoma, M., Jenkins, A., Holland, D., Jacobs, S., 2008. Modelling circumpolar deep water intrusions on the Amundsen Sea continental shelf, Antarctica. Geophys. Res. Lett. 35 (10.1029).

Worby, A., Geiger, C., Paget, M., Woert, M. V., Ackley, S., DeLiberty, T. L., 2008. Thickness distribution of Antarctic sea ice. J. Geophys. Res. 113, C05S92, doi:10.1029/2007JC004254.

Part II

Papers

Paper 1

Paper 2

Paper 3

Paper 4

ISBN xxx-xx-xxxx-xxx-x